



## Shoreline exposure controls teal carbon accumulation in boreal lakes

Ana Lúcia Lindroth Dauner<sup>1</sup>, Max O. A. Kankainen<sup>1</sup>, Sakari Väkevä<sup>2</sup>, Eero Asmala<sup>3</sup>, Marko Järvinen<sup>2</sup>, Karoliina Koho<sup>3</sup>, Tom Jilbert<sup>1</sup>

<sup>1</sup>Environmental Geochemistry Group, Department of Geosciences and Geography, University of Helsinki, Gustaf 5 Hällströmin Katu 2, Helsinki, 00560, Finland

<sup>2</sup>Finnish Environment Institute (Syke), Latokartanonkaari 11, Helsinki, 00790, Finland

<sup>3</sup>Geological Survey of Finland (GTK), Vuorimiehetie 5, P.O. Box 96, Espoo, 02151, Finland

*Correspondence to:* Ana Lúcia Lindroth Dauner ([ana.lindrothdauner@helsinki.fi](mailto:ana.lindrothdauner@helsinki.fi); [anadauner@gmail.com](mailto:anadauner@gmail.com))



10 **Abstract.** Aquatic vegetated ecosystems play an important role in global carbon sequestration. While research on coastal marine environments has expanded in recent decades, freshwater vegetated shorelines remain understudied despite their potential for significant carbon burial. This is especially relevant in boreal landscapes with high numbers of small, shallow lakes. In this study, we quantify organic carbon stocks (mass of carbon per area) in boreal lacustrine vegetated shorelines, so-called *teal carbon* environments. Moreover, we identified the main environmental drivers of carbon storage in these areas.

15 We took 27 sediment cores from three large lakes in Finland with available satellite data of macrophyte coverage. At each site, sediment cores were sampled along a depth transect through macrophyte zones, from the landside towards the waterside. Sedimentary organic carbon (SOC) stocks ranged from 0 to  $40.8 \text{ kg m}^{-2}$ , and showed a large spatial variability among lakes, zones and type of vegetation. We identified grain size as the most significant parameter explaining variability in the size of SOC stocks. Sites dominated by silts and with large SOC stocks were found in sheltered embayments,

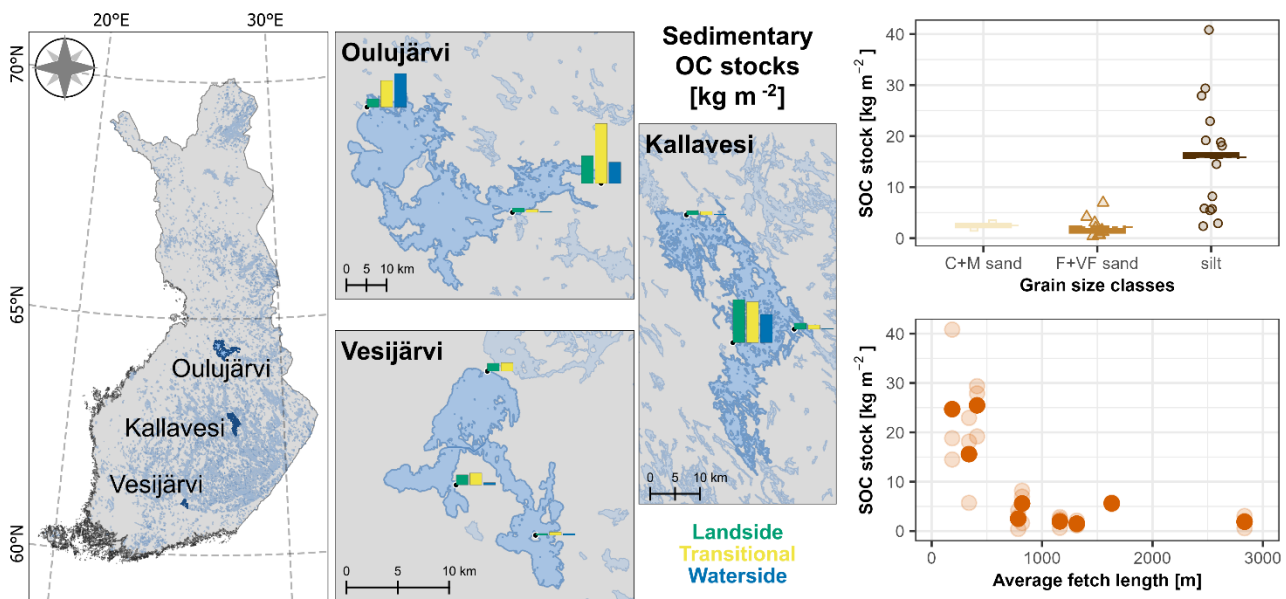
20 independent of proximity to rivers, density of vegetation or slope of the shoreline, implying a strong control of exposure on SOC accumulation. In more exposed areas, vegetation density might play an additional controlling role in SOC accumulation. Accounting for shoreline exposure is crucial for improving regional carbon budget estimates. This study highlights the central role of *teal carbon* ecosystems in carbon cycling in the boreal zone, often characterized by very high densities of lakes.



**Short summary.** Aquatic vegetated ecosystems are important for global carbon sequestration, but freshwater shorelines remain understudied. We found that the sedimentary organic carbon (SOC) stocks ranged from 0 to 40.8 kg m<sup>-2</sup>, with a large spatial variability. Large SOC stocks were found in sheltered areas, with the predominance of fine-grained sediments. In exposed areas, vegetation might also impact SOC accumulation. Accounting for shoreline exposure is crucial for improving 30 regional carbon budget estimates.



**Key figure.** Visual representation of sedimentary organic carbon (SOC) stocks in *teal carbon* environments from three boreal lakes. Grain size (C+M sand = coarse and medium sand, F+VF sand = fine and very fine sand) and average fetch length are the main predictors of high SOC stocks.





## 1 Introduction

In the past decades, the importance of inland freshwater ecosystems in biogeochemical cycles and organic carbon (OC) budget calculations has been increasingly recognized (Cole et al., 2007; Tranvik et al., 2018). Lake and reservoir ecosystems receive a large amount of organic matter from catchment areas and autochthonous production, of which only a portion is transported to adjacent coastal and marine environments. Therefore, despite the relatively small area that they cover, lake ecosystems can sequester large amounts of OC. Recent estimates suggest their OC removal to be in the same order of magnitude as in the open ocean (around  $0.15 \text{ PgC yr}^{-1}$ ; Regnier et al., 2022). OC sequestration may be particularly important in the boreal biome, with a very high density of lakes (Mohamed Anas et al., 2015).

In freshwater ecosystems, the importance of open water sediments for long-term OC burial and storage is well documented (Kortelainen et al., 2004; Cole et al., 2007; Mendonça et al., 2017; Tranvik et al., 2018), but the role of vegetated (flooded) shoreline areas in C storage is less well understood. In coastal marine environments, so-called *blue carbon* areas contribute up to 50 % to the global marine OC burial (Duarte et al., 2005). Similarly, shallow vegetated areas in lacustrine environments, so-called *teal carbon* environments (Nahlik and Fennessy, 2016), may potentially play an important role in cycling and burial of organic matter. The ability of such vegetated ecosystems to sequester and remove OC remains poorly determined, even though the importance of freshwater wetlands has started to gain attention in the last decade (Taran et al., 2023). The recent increased awareness of freshwater vegetated areas has been partly boosted by the Ramsar conventions (Convention on Wetlands, 2021), which recognized their ecosystem services and benefits to humans. Despite this, OC stocks and fluxes in these environments have not yet been incorporated into the most recent conceptualizations of the continental OC cycle (Grasset et al., 2025; Regnier et al., 2022), due to lack of data and mechanistic understanding of the processes controlling OC cycling.

In this paper, we focus on aquatic macrovegetation (macrophytes) whose life-form is helophytic, i.e., that are anchored in bottom mud and have emergent stems and overwintering root systems (Bornette and Puijalon, 2009). OC stocks and sequestration rates in wetlands are expected to be highly variable because of the broad suite of natural and anthropogenic factors controlling the accumulation and storage of organic material (Tangen and Bansal, 2020). However, some general trends have been identified. For example, in marine saltmarshes formed by common reed *Phragmites australis*, the waterside zone of the macrophyte belt tends to accumulate less OC than the landside (Buczko et al., 2022). A similar pattern has also been observed in freshwater wetlands (Bernal and Mitsch, 2012; Tangen and Bansal, 2020; Taran et al., 2023; Silan et al., 2024), implying a role for exposure in determining the eventual accumulation of organic matter in sediments, whereby growth of dense macrophyte vegetation promotes physical trapping of fine-grained organic-rich material from the water column. Species composition and density of the macrophyte patches may also play a role in determining the magnitude of OC storage (Bernal and Mitsch, 2012). However, few systematic studies have been carried out to understand the relative role of the numerous parameters that control the amount of OC stored in the sediments of *teal*



70 *carbon* environments. Quantifying variability in OC storage and sequestration among the wetland types, within and between geographical regions, has been identified as a high priority (Carnell et al., 2018). The closest blue carbon analogue for Finnish lakes would be found on the Baltic Sea coast, because of climatic similarity, overlap in dominant macrophyte species, and the low overall salinity of the Baltic Sea. Vast *Phragmites* areas are found especially in undisturbed lagoons and wetlands of southern Baltic Sea countries (Buczko et al., 2022), but there the  
75 milder climate and lack of seasonal ice cover supports longer growth seasons, less physical disturbance, and, potentially, higher carbon accumulation than in Finnish lakes.

In order to better understand the OC sink potential of *teal carbon* environments of boreal lakes, we studied the factors controlling OC stocks in shoreline areas of three large lakes in Finland. The studied ecosystems are dominated by common reed (*Phragmites australis*) with additional contributions of horsetails (*Equisetum* spp.) and sedges (*Carex* spp.). Through comprehensive analysis of sediment samples and environmental variables, we (i) quantify the magnitude of sediment OC stocks in shallow vegetated areas of the study lakes, (ii) identify the main parameters governing these, and (iii) compare our new OC stock estimates with those of other freshwater and marine environments to assess the relative magnitude of boreal *teal carbon* accumulation. Based on these objectives, we hypothesized that (i) the presence and abundance of macrophytes are likely to promote the accumulation of OC in  
85 *teal carbon* environments, and that (ii) *teal carbon* environments can have OC stocks comparable to coastal *blue carbon* environments in similar latitudes, but shorter growing seasons and seasonal ice cover might make the lake environments less efficient accumulators in practice.

## 2 Material and Methods

### 2.1 Study Area

90 The studied lakes span across a 400-km latitudinal gradient in Finland, all within the boreal zone (Figure 1). The lakes and sampling sites were chosen based on their water quality, using aerial and satellite images showing the evidence of extensive areas of macrophyte vegetation on Finnish lakes, and accessibility of the sampling sites (Figures S1 to S9b).

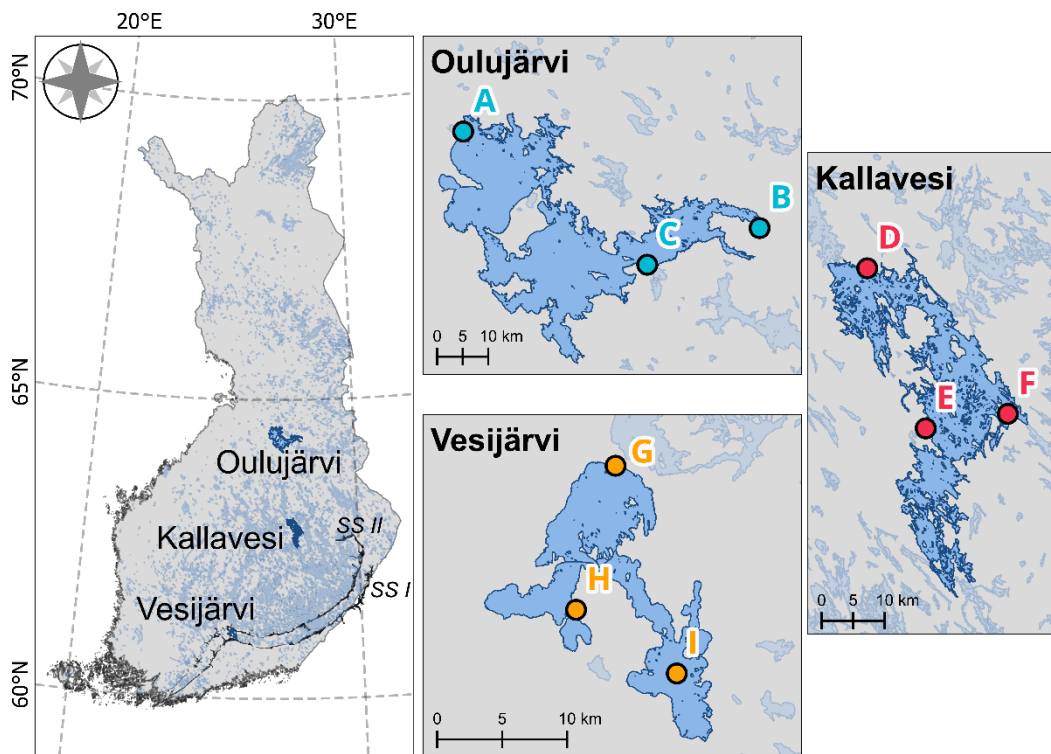


**Figure 1.** Sampling sites (A to I). At each site, a depth transect was sampled, yielding 9 sediment cores per lake. The Finland shapefile was obtained from DVV (2023). SS I and SS II indicate the positions of ice marginal sand ridges *Salpausselkä* I and II, respectively (Repo and Tynni, 1971).

95 The clearwater and mesotrophic Lake Vesijärvi is the smallest and southernmost lake sampled in the study, while the humic and oligotrophic Lake Kallavesi is located in central Finland, and the humic Lake Oulujärvi with large (2.7 m) water level regulation is the largest and northernmost lake (Tables 1 and S1). All three lakes are located north of the youngest of the *Salpausselkä* ice marginal sand ridges that are among the most conspicuous glacial formations in Finland (Rainio et al., 1995). The *Salpausselkä* I and II formations were laid down during the Younger Dryas cold climatic period, 100 and constitute a zone approximately 20-50 km wide and 600 km long across southern Finland, which is composed mainly of glaciofluvial gravel and sand (Tikkanen, 2006; Rainio et al., 1995). In the regions north of the ice marginal formations, large deposits of gravel and sand are also found in eskers, representing the locations of subglacial streams and oriented approximately in the direction of glacial movement (Tikkanen, 2006; Hyvärinen, 1973). Other widespread landforms dating from the deglaciation and subsequent land uplift are large clay plain and mires (Tikkanen, 2002). This mosaic of surficial 105 materials contributes to the soils and thus also the freshwater sediments in the regions of the three study lakes.

Lake Vesijärvi is located between *Salpausselkä* I and II formations and, thus, the region is mainly covered by surficial deposits of glaciofluvial sands (GTK, 2024) (Figure S10). Lake Kallavesi is located in a region with a notable presence of eskers (Glückert, 1974) and its surroundings are mainly covered by bedrock outcrops, sandy eskers and mixed soil (GTK,



2024) (Figure S10). Because of its northern location, lake Oulujärvi's surroundings also present some sandy eskers in the  
110 surficial deposits, but are mainly characterized by mixed soils and a thick peat layer (GTK, 2024) (Figure S10).

**Table 1. Description of sampled lakes.**

Notes:

<sup>1</sup> Vesijärvi – Kairesalo and Vakkilainen (2004), Kallavesi – Noori et al. (2022), Oulujärvi – Turunen et al. (2022);

<sup>2</sup> considering the last 30 years (FMI database, 2024);

<sup>3</sup> Syke (2019)

<sup>4</sup> Vesijärvi – Kankaala et al. (2004), Kallavesi – Partanen et al. (2006), Oulujärvi – Keränen et al. (1992);

<sup>5</sup> Syke (2025a)

<sup>6</sup> Vesijärvi and Kallavesi – Syke (2025b), Oulujärvi – Järvi-meriwiki (2025)

Lake	Vesijärvi	Kallavesi	Oulujärvi
Area [km <sup>2</sup> ]	110	478	902
Average depth [m] <sup>1</sup>	6	10	8
Max depth [m] <sup>1</sup>	42	75	35
Summer monthly average air temperature [°C] <sup>2</sup>	17.7	17.5	16.3
Winter monthly average air temperature [°C] <sup>2</sup>	-5.8	-8.0	-9.4
Ecological status <sup>3</sup>	moderate to good	moderate to good	good
Main shoreline vegetation <sup>4</sup>	common reed ( <i>Phragmites australis</i> )	common reed ( <i>Phragmites australis</i> ) and horsetail ( <i>Equisetum</i> sp.)	common reed ( <i>Phragmites australis</i> ) and horsetail ( <i>Equisetum</i> sp.)
Main land use type in the catchment area <sup>5</sup>	boreal forest (51 %) and arable land (18 %)	boreal forest (73 %)	boreal forest (78 %)
Main anthropogenic pressure <sup>6</sup>	diffuse loading (agriculture), storm water, summer house settlements	point source loading, diffuse (agriculture)	hydromorphological alteration (water level regulation)

## 2.2 Sampling procedure

The sampling campaign was conducted in August 2023 in the vegetated shoreline areas of Vesijärvi, Kallavesi and Oulujärvi. From each lake, three sites, each including a depth transect of 3 zones, were sampled yielding a total of nine  
115 sediment cores per lake (Figure 2). At each site, sampling was performed along a depth transect across the vegetation patch (one core from each of the following zones: landside, transitional, waterside; Table S2; Figures 2 and S1 to S9d). Each site was selected based on existing evidence of macrophyte patches from satellite (Koponen et al., 2022) and aerial (Finnish National Geoportal (Orthophotos), 2023) images (Figures S1 to S9b), and aligned with sites where previous macrophyte campaigns had also been carried out. Regular grids (10 × 10 m or 5 × 5 m, depending on the size of the vegetation patch)  
120 were created for each macrophyte patch. Based on satellite images (Koponen et al., 2022), the closest grid points to the lake shoreline were selected as potential starting points (i.e., the “landside” sampling point) of each transversal transect. For each sampling site (vegetation patch), the starting point was randomly selected using the “Random selection” tool of QGis (QGIS



Development Team, 2024) (Figures S1 to S9c). The starting points were always within the vegetation patch but could be either submerged or waterlogged. “Transitional” and “waterside” sampling points followed a transect perpendicular to the shoreline across the vegetation patch (Figures S1 to S9d). “Waterside” sampling points were the furthest grid points from the starting points (“landside”) within the vegetation patch based on satellite images. “Transitional” sampling points were selected as the middle grid points between “landside” and “waterside” sampling points.

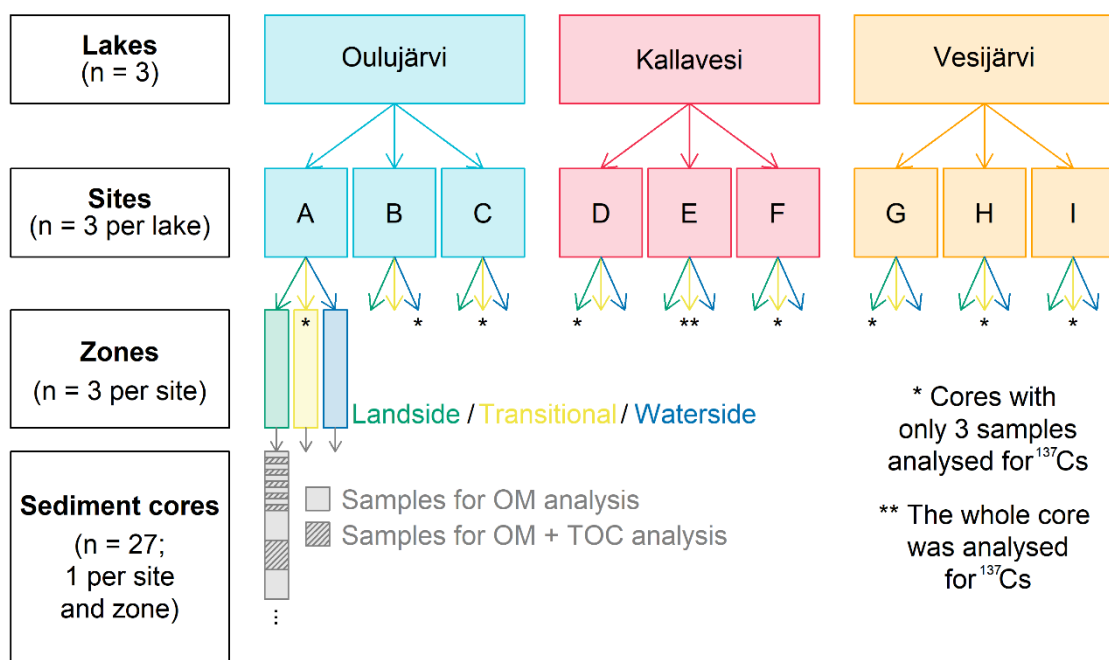


**Figure 2. Schematic diagram of the sampling design and the scales of the studied spatial variability.**

130 Sediment sampling was performed using a combination of two hand-held coring systems: a short piston corer (0.5 m length, 4 cm internal diameter) and a long box corer (100 cm length, 8 x 8 cm cross-section area). The corers were inserted into the sediments and pushed down until 1 m was reached, or until no further penetration was possible. Final depths obtained varied by site and zone (20–100 cm), and were mostly determined by the transition from organic-rich surface material to more compacted organic-poor material deeper in the core. Each of the 27 cores was sliced at 2 cm resolution in the first upper 20 cm, and 10 cm resolution until the bottom of the core. Sediment cores that had a clear compositional transition (e.g. from fine grained organic rich sediments to organic poor clay) below the top 20 cm were sliced at 5 cm resolution until reaching that transition, and then at 10 cm resolution downwards.

135 Samples (n = 359) were bagged and kept refrigerated until weighed in the laboratory. They were then frozen, freeze-dried and weighed again to determine dry mass [g] and water content [%]. Because some of the samples contained large rhizomes



140 and pebbles, each sample was broken up with mortar and pestle and sieved through a 2-mm mesh for further analysis. The fraction retained in the sieve ( $> 2$  mm) was weighed, and visually categorized as mainly “biogenic”, “lithogenic” or a “mixture” of both (Figures S11 to S13). For the purposes of visualization, we classified the sieved samples ( $< 2$  mm) into three categories based on grain size (d50, section 2.3) and total organic carbon (TOC) content: “sands” ( $d50 \geq 62.5 \mu\text{m}$ ), “OM-poor (grey) silts” ( $d50 < 62.5 \mu\text{m}$  and  $\text{TOC} \leq 5\%$  dry weight (dw)) and “OM-rich silts” ( $d50 < 62.5 \mu\text{m}$  and  $\text{TOC} > 5\%$  dw)).

145 In each zone, in addition to the sediment core, vegetation stems for all macrophyte species were counted and identified in a quadrat of  $1 \text{ m}^2$ .

### 2.3 Laboratory analyses

150 Organic matter (OM) content was measured by dry combustion at  $550^\circ\text{C}$  (loss on ignition, LOI) using a LECO TGA701 analyser (LECO Corp., St Joseph, MI, USA; precision of 0.02 % RSD – relative standard deviation), while TOC was determined by dry combustion using a LECO CN828 analyser (LECO Corp., St Joseph, MI, USA). TOC limit of detection was 0.000017 %. OM was measured in all samples, whereas TOC was determined in 173 out of 359 samples taken alternately in each of the sediment cores, i.e. at every other sample (Figure 2). These data were used to estimate TOC content in the remaining 186 samples by linear regression (a conversion factor of 0.44;  $r^2 = 0.98$ ) (Fig. S14).

155 Grain size was measured on the sieved and inorganic fraction of the sediments using a Microtrac FlowSync particle size analyser and is reported as % of fine-grained sediments. The precision of measurement based on replicates from an in-house sediment reference sample was 3 %.

The longest (0.9 m) sediment core (lake Kallavesi, Site E, zone transitional) was selected to be used as a reference core for sediment dating. Additionally, three samples within single sediment cores from the remaining eight sites were also selected 160 (Figure 2). All selected samples were analysed for  $^{137}\text{Cs}$  activity using BrightSpec gamma spectrometer (3600 s counting time, Geological Survey of Finland). We prospected for a single major peak in the profile assumed to correspond to the 1986 Chernobyl nuclear accident (Ojala et al., 2017), as evidence for continuous sediment accumulation in the reference core.

### 2.4 Data conversions and analyses

165 Dry bulk density (DBD) was determined from the sediment density corrected by organic matter content (Eq. 1), the water content and the sample volume. Wet and dry sample weights were used to calculate the sediment content [% relative to sample weight] (Eq. S1 and S2), which was in turn converted into sediment volume [% relative to sample volume] and porosity  $\Phi$  [fraction of 1] (Eq. S3 to S5). Finally, porosity [fraction of 1], sediment density [ $\text{g cm}^{-3}$ ] and sediment content [%] were used to calculate wet bulk density (WBD) (Eq. 2) and dry bulk density (DBD) (Eq. 3).

$$\text{Sediment density } \left[ \text{g/cm}^3 \right] = 1.4 * \left( \frac{\text{OM}}{100} \right) + 2.65 * \left( 1 - \frac{\text{OM}}{100} \right), \quad (1)$$



170 where  $1.4 \text{ g cm}^{-3}$  is the assumed density for sediments rich in OM and  $2.65 \text{ g cm}^{-3}$  is the grain density of quartz (Pajunen, 2000; Burdige, 2006).

$$\text{WBD} \left[ \text{g/cm}^3 \right] = (\Phi * 1) + \left( (1 - \Phi) * \text{Sediment density} \left[ \text{g/cm}^3 \right] \right) \quad (2)$$

$$\text{DBD} \left[ \text{g/cm}^3 \right] = \frac{\text{Sediment content} [\%]}{100} * \text{WBD} \left[ \text{g/cm}^3 \right], \quad (3)$$

175 where  $\Phi$  = volumetric porosity. TOC inventory for a given sample [g] was calculated multiplying the TOC content [%] by the DBD [ $\text{g cm}^{-3}$ ] and the sample volume [ $\text{cm}^3$ ]. For the C stock calculations, only samples with  $> 1\%$  OM were considered (Kortelainen et al., 2004). The TOC inventories were summed for all sampled depths to obtain a cumulative inventory [g] per core. Lastly, the cumulative TOC inventories [g] were divided first by 1000 (to obtain data in kg) and then by the coring device cross-section areas to obtain sedimentary organic carbon (SOC) stocks [ $\text{kg m}^{-2}$ ] (Eq. 4a).

$$\text{SOC stock} \left[ \text{kg/m}^2 \right] = \frac{\sum_{\text{core bottom}}^{\text{core top}} (\text{TOC} * \text{DBD} * \text{depth}) * 1000}{\text{area}} \quad (4a)$$

$$180 \text{ SOC stock}_{(0-20)} \left[ \text{kg/m}^2 \right] = \frac{\sum_{20 \text{ cm depth}}^{\text{core top}} (\text{TOC} * \text{DBD} * \text{depth}) * 1000}{\text{area}}, \quad (4b)$$

where SOC stock is sedimentary organic carbon stock [ $\text{kg m}^{-2}$ ], TOC is total organic carbon concentration [%] in the samples (where OM  $> 1\%$ ), DBD is the dry bulk density of each sample [ $\text{g cm}^{-3}$ ], depth is the thickness of sampled material [cm] and area is the cross-section areas of the coring devices [ $\text{m}^2$ ].

185 To remove the effect of different core lengths in the SOC stock calculation, SOC stocks were also calculated for the top 20 cm of each core (Eq. 4b). This depth (20 cm) was selected as it is the length of the shortest core (landslide zone of site D in Kallavesi). Additionally, SOC accumulation values were calculated normalizing SOC stocks by the depth of the organic-rich layer in each sediment core (Eq. 5).

$$\text{SOC accumulation} \left[ \frac{\text{kg/m}^2}{\text{cm}} \right] = \frac{\text{SOC stock} \left[ \text{kg/m}^2 \right]}{\text{depth of organic-rich layer} [\text{cm}]} \quad (5)$$

190 where SOC stocks [ $\text{kg m}^{-2}$ ] were calculated in Eq. 4a and the depth of the organic-rich layer [cm] is defined by samples containing more than 1 % OM (Kortelainen et al., 2004).

Maps were produced using QGIS version 3.28.4 (QGIS Development Team, 2024), plots and statistical analyses were performed using R version 4.3.3 (R Core Team, 2024), and package *ggplot2* was used for graphics (Wickham, 2016). TOC content and SOC stock estimates were log-transformed prior to statistical analysis to meet assumptions of normality and homogeneity of variance. One-way analyses of variances (ANOVA) were computed to compare grain size distribution (% of fine-grained sediments), TOC contents and SOC stock estimates across ecosystems, considering categorical parameters. For the grain size distribution, lakes and zones were used as categorical parameters. For the TOC content analysis, lakes, zones and grain-size classes were used as categorical parameters. For the SOC stock analysis, the used categorical parameters were



lakes, zones, grain-size classes and macrophyte types. A post hoc Tukey Pairwise Comparison was performed to identify groups that differ significantly from each other.

200 Additionally, SOC stock estimates were also compared to environmental numerical parameters, i.e., density of macrophyte stems [ $\text{stems m}^{-2}$ ], water depth [m], slope of each site (calculated as the distance between the landside and waterside sampling locations divided by the difference in their depth), and the average fetch length. For each sampling site (A–I), the distance to the nearest shoreline (either lake shoreline or islands) was calculated considering 48 angles (from 0 to  $345^\circ$ , by  $15^\circ$  increments) (Murtojärvi et al., 2007; Hayes, 1996). The average of these 48 distances was considered as the “average fetch length”. R packages *terra* (Hijmans et al., 2024) and *waver* (Marchand and Gill, 2023) were used to import shapefiles into R and calculate the fetch lengths, respectively. Lastly, a generalized linear model (GLM; using multiple regression and family gamma) was employed to examine if there were significant relationships between our SOC stock estimates and the environmental numerical parameters (density of macrophyte stems, water depth, slope of each site, and the average fetch length using R package *glm2* (Marschner and 205 Donoghoe, 2022). The data was tested for multicollinearity using the variance inflation factor (VIF) analysis and they did not present multicollinearity.

210

### 3 Results

#### 3.1 Evidence for long-term sediment accumulation

The signal of the 1986 Chernobyl nuclear accident was not clearly visible in the  $^{137}\text{Cs}$  profiles of our samples (Figure S15). 215 The maximum activity observed in the longest core was around  $160 \text{ Bq kg}^{-1}$ , while peak values can reach up to  $4\,800 \text{ Bq kg}^{-1}$  dry wt in deeper areas of the studied lakes (Junna et al., *in press*). The low  $^{137}\text{Cs}$  signal values observed in the *teal carbon* areas imply mixing and removal of material, either by in-situ bioturbation (e.g. from roots or sediment dwelling invertebrates) or from physical action. The lack of clear  $^{137}\text{Cs}$  profile with a peak value suggests that there is no net sediment accumulation at our study sites, and the shoreline areas do not act as permanent deposition locations for carbon, but rather 220 zones of temporary carbon storage. This interpretation is supported by clear unconformities in most cores between a distinct surface layer rich in organic material and basal organic-poor material (Figures S11 to S13, and S16). As such, the calculation of the sediment and carbon mass accumulation rates were not possible and instead we based our interpretation and discussion on stock estimates (mass per unit area) of carbon.

#### 3.2 Grain size and organic matter content

225 The sediments from all cores can be classified as organic-poor sands, organic-rich silts, or as organic-poor silts. The grain size ( $d_{50}$ ) varied between 7 and  $819 \mu\text{m}$  while the percentage of fine-grained sediments (silt + clay) varied between 0 and 95 % (Figure S17; Table 2). Lakes Kallavesi and Oulujärvi had a larger fraction of fine-grained sediments (means and median between 50 and 65 %) than lake Vesijärvi (30 % and 24 %, respectively) (Figure 3a). There was a clear difference also



230 between shoreline zones (Figure 3b). Larger fractions of fine-grained sediments were observed in the landside and transitional zones (means and median between 47 and 62 %), while samples from the waterside presented a coarser grain size distribution, with fine-grained sediments presenting a mean of 37 % and a median of 28 %.

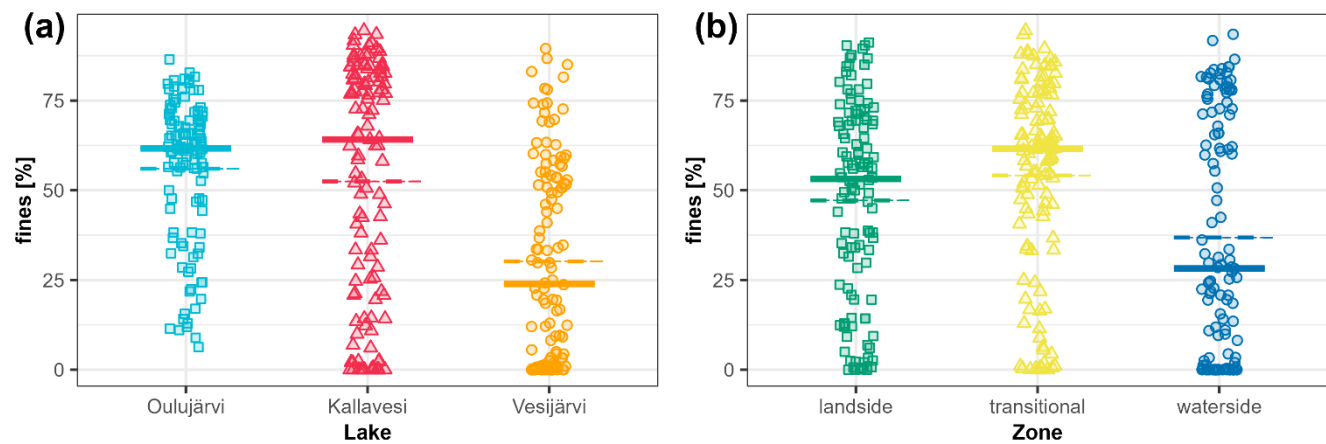


Figure 3. Grain size distribution (% of fine-grained (silt + clay) sediments) grouped by (a) lakes and (b) zones. The dashed horizontal lines indicate the mean, and the continuous bold horizontal lines indicate the median. Significant differences were observed among the three lakes (ANOVA  $F$ -value = 30.40;  $p$ -value < 0.05), and the three shoreline zones (ANOVA  $F$ -value = 10.61;  $p$ -value < 0.05), with the samples from lake Vesijärvi and the waterside zone containing overall less fine-grained sediments (Tukey test results in Table S3).



**Table 2. Fraction of fine-grained sediments, mean grain-size class, total organic carbon (TOC), SOC stocks by sediment core, using two different approaches (whole sediment core vs top 20 cm), core length, depth of organic-rich layer (samples with organic matter content > 1 %) and SOC accumulations in the organic-rich layer. Fraction of fine-grained sediments [%] and TOC [% dw] are presented as “minimum – maximum (median value)”. Abbreviations: C+M sand = coarse and medium sands; F+VF sand = fine and very fine sands.**

Lake	Site	Zone	Fine-grained sediments [%]	Mean grain size class	TOC [%]	SOC stocks <sup>a</sup> [kg m <sup>-2</sup> ]	SOC stocks (0-20) <sup>b</sup> [kg m <sup>-2</sup> ]	Core length [cm]	Depth of organic-rich layer [cm]	SOC accumulation in the organic-rich layer <sup>c</sup> [kg m <sup>-2</sup> cm <sup>-1</sup> ]
Oulujärvi	A	landsid	56.1 - 75.4 (68.8)	silt	0.3 - 33.1 (2.9)	5.72	3.92	40	40	0.14
		transitional	44.9 - 80.9 (70.9)	silt	0.5 - 27.8 (9)	18.12	6.32	40	40	0.45
		waterside	60.1 - 82.8 (78)	silt	12.8 - 25.8 (16.2)	22.92	7.72	50	50	0.46
	B	landsid	52.7 - 69.6 (60)	silt	2 - 38.2 (26.2)	18.80	7.88	50	50	0.38
		transitional	58.6 - 73 (63.4)	silt	20.2 - 41.6 (35.5)	40.81	6.68	65	65	0.63
		waterside	55.4 - 86.5 (65.9)	silt	0.6 - 34.8 (28.4)	14.50	9.21	50	50	0.29
	C	landsid	32.5 - 71.3 (46.8)	F+VF sand	0.2 - 4.4 (1.3)	3.06	3.06	70	20	0.15
		transitional	6.3 - 66.6 (21.8)	F+VF sand	0 - 10.2 (0.4)	2.04	2.04	50	16	0.13
		waterside	11 - 47.2 (25.8)	F+VF sand	0.1 - 8.6 (0.1)	0.58	0.58	40	4	0.15
Kallavesi	D	landsid	0 - 72.3 (0.4)	C+M sand	0.4 - 33.2 (1.1)	2.84	2.84	20	18	0.16
		transitional	40.6 - 94.5 (61.9)	silt	0 - 21.8 (0.2)	2.38	2.11	43	32	0.07
		waterside	0 - 10.9 (0)	F+VF sand	0.1 - 9.1 (0.1)	0.67	0.67	30	16	0.04
	E	landsid	75.1 - 91.2 (84.7)	silt	14.3 - 39.4 (31.6)	29.36	8.86	70	70	0.42
		transitional	76.9 - 89.5 (83.7)	silt	3.3 - 32.1 (20.7)	27.89	9.13	90	90	0.31
		waterside	72.7 - 93.5 (81.5)	silt	2.4 - 27.6 (23.4)	19.17	4.39	80	80	0.24
	F	landsid	2.1 - 90.4 (13.3)	F+VF sand	0 - 5 (0.4)	4.19	1.33	50	50	0.08
		transitional	33.4 - 64.6 (59.1)	silt	0.2 - 1 (0.7)	2.91	1.66	35	35	0.08
		waterside	9.9 - 42.5 (24.7)	F+VF sand	0 - 0.7 (0.1)	0.42	0.42	44	16	0.03
Vesijärvi	G	landsid	0.6 - 78.1 (50.7)	silt	0 - 38.9 (0.6)	5.45	3.72	65	60	0.09
		transitional	0.7 - 86.8 (63.3)	silt	0 - 32.5 (17)	5.81	4.45	50	50	0.12
		waterside	0 - 1.3 (0)	F+VF sand	0 - 0.3 (0.2)	0.00	0.00	35	0	0.00
	H	landsid	9.4 - 83.1 (49.3)	F+VF sand	0.3 - 24.9 (1)	6.97	2.95	70	70	0.10



		transitional	25 - 69.7 (52.5)	silt	0.2 - 24.2 (16)	8.18	3.81	60	60	0.14
		waterside	0 - 50.7 (14)	F+VF sand	0 - 1.4 (0.2)	1.63	0.64	60	40	0.04
I	waterside	landsid	0.6 - 89.5 (34.4)	F+VF sand	0.1 - 1.7 (0.4)	1.24	1.24	40	20	0.06
		transitional	0 - 36.7 (0.6)	C+M_sand	0 - 0.5 (0.2)	2.12	0.56	50	50	0.04
	transitional	landsid	0 - 59.9 (3.9)	F+VF sand	0.1 - 7.2 (0.3)	1.19	1.19	32	20	0.06
		waterside								

<sup>a</sup>: SOC stocks [kg m<sup>-2</sup>] considering whole sediment cores.

<sup>b</sup>: SOC stocks<sub>(0-20)</sub> [kg m<sup>-2</sup>] considering samples from only the top 20 cm of each core.

<sup>c</sup>: SOC accumulation [kg m<sup>-2</sup> cm<sup>-1</sup>] considering whole sediment cores. SOC stock values [kg m<sup>-2</sup>] were divided by the depth [cm] of the organic layer in each core.

235

Most of the sediment cores presented a top layer typically rich in organic matter content [% dw] that was overlying sandier sediments and/or organic-poor silts (Figures S11 to S13, and S16), both poor in organic matter (Figure 4). The top 30 cm encompasses the entire OM-rich layer in many cases, and only at sites A, B (lake Oulujärvi) and E (lake Kallavesi) was the whole sediment core filled with organic-rich material (Figures S11 and S12). The percentage of TOC across all samples 240 varied between 0 and around 40 % dw in each of the three lakes, and the medians were 1.0 % dw, 0.4 % dw, and 9.8 % dw, respectively (Table 2). Significant differences were observed among the three lakes (ANOVA F-value = 18.62; *p*-value < 0.05), shoreline zones (ANOVA F-value = 6.441; *p*-value < 0.05), and grain-size classes (ANOVA F-value = 83.73; *p*-value < 0.05), with the samples containing silts presenting overall larger TOC content (Tukey test results in Table S4).

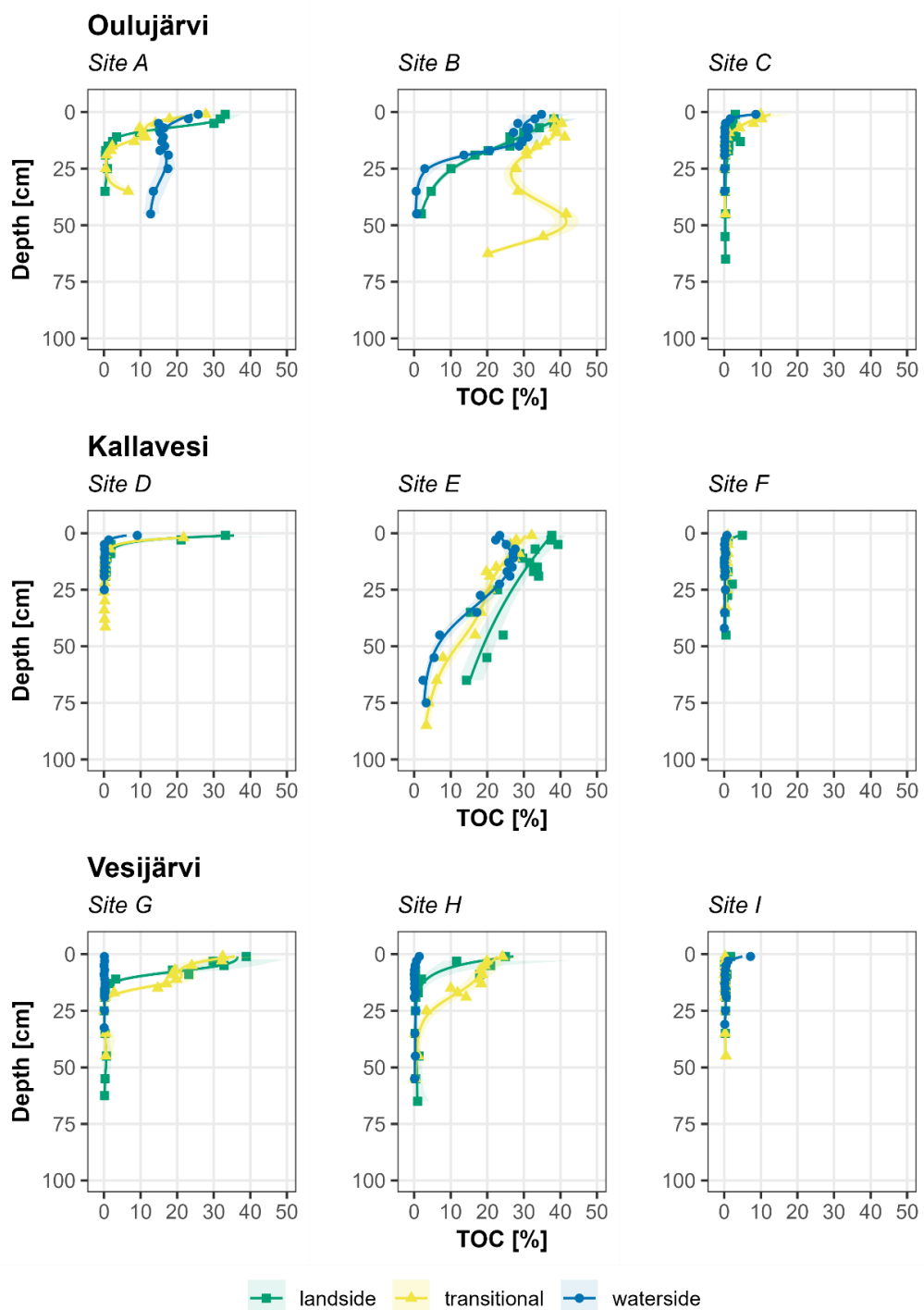


**Figure 4.** Vertical profiles of total organic carbon (TOC) in % dw.



### 3.3 Organic carbon stocks

The whole core SOC stocks varied between 0 and 40.8 kg m<sup>-2</sup>, with a large variability being observed between lakes and sites (Figure 5a). Larger stocks were generally observed in Oulujärvi, and smaller stocks in Vesijärvi (Figure 5b). For the shoreline zones, smaller SOC stocks were observed on the waterside (Figure 5c). Significant differences were observed

250 among different types of vegetation (ANOVA F-value = 5.102; *p*-value < 0.05), with the sites dominated by “non-*Phragmites*” vegetation presenting generally larger SOC stocks (Figure 5e). As the ANOVA results for TOC content [% dw], the most significant differences between SOC stocks were observed among cores of different grain size classes (ANOVA F-value = 14.650; *p*-value < 0.05), with larger amounts of SOC stock observed only in the presence of silts (Figure 5d) (Tukey test results in Table S5).

255 Similar patterns were observed when only the top 20 cm were considered for the SOC stock calculation (Figure S18) and for SOC accumulation (Figure S19), with larger amounts of SOC stock (0-20) and SOC accumulation estimates being observed only in the presence of silts and most commonly in sites dominated by “non-*Phragmites*”. Their geospatial patterns were also very similar, with slightly larger mean and median values being observed in Oulujärvi and lower values in the waterside.

260

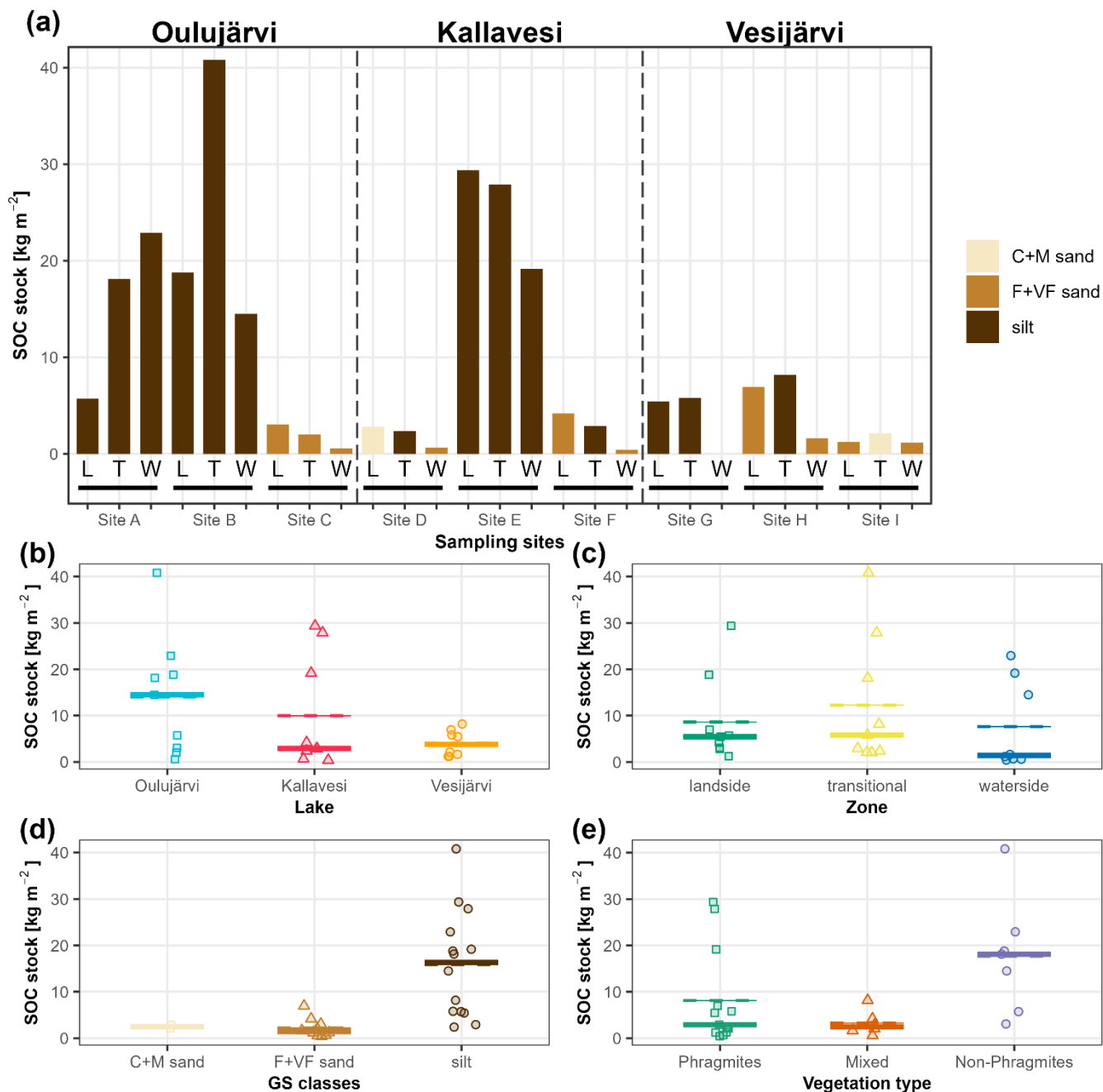


**Figure 5.** Sedimentary organic carbon (SOC) stocks [ $\text{kg m}^{-2}$ ] of the sediment cores (a) and grouped by lakes (b), shoreline zones (c), grain size classes (d) and vegetation type (e). Stock estimates consider only samples with  $> 1\%$  of organic matter. In panels (b) to (e), the dashed horizontal lines indicate the mean, and the continuous bold horizontal lines indicate the median. Abbreviations: L = landside zone; T = transitional zone; W = waterside zone; C+M sand = coarse and medium sands; F+VF sand = fine and very fine sands. In (a), the bars are coloured according to the grain size averaged through the whole sediment core.



### 3.4 Environmental predictors of carbon stocks

To assess the relationship between environmental predictors and SOC stocks, we compared our cumulative SOC stocks with the density of macrophyte/helophyte vegetation, water depth, slope of each site, and average fetch length (Figure 6). When 265 all sites were considered together, the stem density does not seem to be a key parameter explaining carbon accumulation on lakes shorelines (Figure 6a). However, when lakes and zones are considered separately (Fig. S20), the vegetation density becomes somewhat important on the waterside zone, and in lakes Kallavesi and Vesijärvi ( $r^2 > 0.5$ ), with higher stem densities corresponding to higher SOC stocks.

For water depth and slope, large SOC stocks ( $> 10 \text{ kg m}^{-2}$ ) were observed across the entire sampled range, from shallow (< 270 0.4 m) to deep (< 1.0 m) sites (Figure 6b), and from gradual (slope index  $> 250$ ) to steep (slope index  $< 50$ ) areas (Figure 6c). The average fetch length, on the other hand, presented the clearest pattern with SOC stocks, with estimates larger than 10  $\text{kg m}^{-2}$  being observed only when fetch lengths were smaller than 500 m (Figure 6d). It was also the most significant (t-value = 4.788;  $p$ -value < 0.05) component in our generalized linear model (Table S6).

When considering only the top 20 cm for the SOC stock calculations or SOC accumulation, the same relationships were 275 observed, with larger values being observed only when the average fetch length was smaller than 500 m (Figures S21 and S22). The similarity between the results reinforces the robustness of using the whole core for the SOC stock calculation.

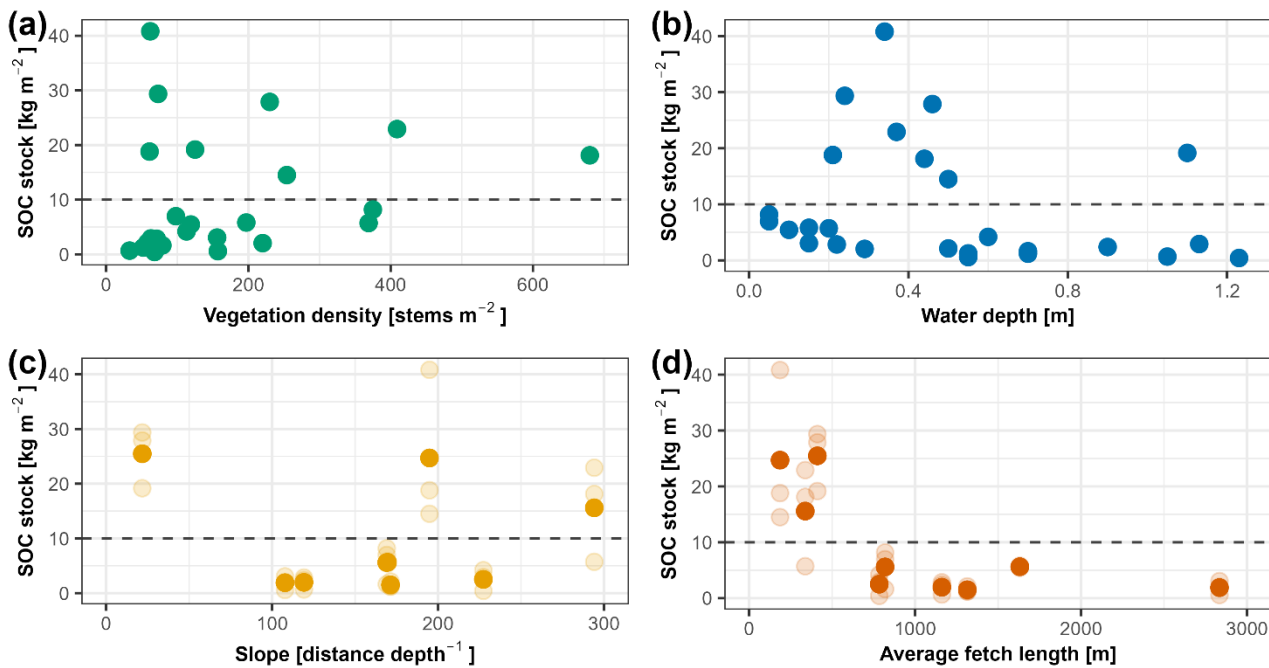


**Figure 6.** Relationship between sedimentary organic carbon (SOC) stocks [ $\text{kg m}^{-2}$ ] and environmental parameters: (a) vegetation density [number of helophyte stems, in  $\text{stems m}^{-2}$ ], (b) water depth [m], (c) slope (calculated as the distance between the landside and waterside sampling locations divided by the difference in their depth), (d) and the average fetch length [m]. In plots (c) and (d), the translucent points indicate the SOC stocks per zone (landside, transitional, waterside) in each site (A to I), while the opaque points indicate the average SOC stock estimates in each site.

## 280 4 Discussion

### 4.1 Grain size controls TOC content and SOC stocks

All three SOC calculations (SOC stocks [ $\text{kg m}^{-2}$ ], SOC stocks<sub>(0-20)</sub> [ $\text{kg m}^{-2}$ ] and SOC accumulation [ $\text{kg m}^{-2} \text{ cm}^{-1}$ ]) presented the same spatial distribution (Table 2), with the highest values being observed in sites A, B (Oulujärvi) and E (Kallavesi), and the lowest in site I (Vesijärvi).

285 When compared with the sedimentological parameters, both TOC content [% dw] and SOC stocks [ $\text{kg m}^{-2}$ ] showed a strong dependency on the grain size (Figures S23 and 5d, respectively). Overall, higher TOC contents ( $> 10\% \text{ dw}$ ) were observed only when the proportion of fine-grained sediments exceeded 50 %. This association is well known, due to the higher specific surface area of lower-grain size materials allowing more OM to be sorbed on the particle surfaces (Keil et al., 1994; Keil and Cowie, 1999). Additionally, OM is more likely to be transported and sedimented 290 with fine inorganic materials due to the hydrodynamics of the environment, i.e., a relatively quiescent setting will



have more fine-grained sediments and more OM sedimentation (Milliman, 1994). Lastly, fine-grained sediments tend to have smaller pore spaces, which might hinder microbial degradation (Bianchi, 2007).

Interestingly, the relationship between TOC content and grain size varied between the studied lakes (Figure S23). Because Vesijärvi is located between the two ice-marginal ridges *Salpausselkä* I and II, most of its surficial deposits are sands and 295 thus, there is less fine-grained material that can be discharges to the lake. Kallavesi and Oulujärvi, on the other hand, are located further north and more influenced by the input of reworked glaciolacustrine clays (Lunkka et al., 2024). This likely causes the two latter lakes to receive more fine-grained sediments. Additionally, the water level of Oulujärvi has been altered in the last decades, which might have impacted the sediment input to the lake.

#### 4.2 Environmental controllers of fine-grained sediments and SOC stocks

300 As pointed out by Tangen and Bansal (2020), SOC stocks are highly variable in space because of the suite of natural and anthropogenic controlling factors. Our SOC stock estimates presented a large spatial variability, ranging from zero to more than 40 kg m<sup>-2</sup> (Figure 5a), and were mainly controlled by the sediment grain size (Figure 5d). Several environmental parameters could influence the entrapment of fine-grained sediments, such as the presence of vegetation acting as barriers for the water flow and mixing, promoting deposition of particulate matter (Leonard and 305 Luther, 1995), and the exposure of the shoreline to waves and currents, which can erode the deposited material (van Rijn, 1993).

Macrophyte presence can promote sediment deposition either through sediment adhesion to vegetation or by attenuating vegetation-induced hydrodynamics (Li and Yang, 2009). However, the role of specific species promoting sediment deposition is not clear (Nikora et al., 2008; Leonard et al., 2002). In our study, we did not observe any general pattern 310 between SOC stocks and type of vegetation, with high SOC stocks being observed both in sites covered only by *Phragmites* and in sites without *Phragmites*, dominated by *Equisetum* spp. and *Carex* spp. (Figure 5e).

Fine-grained sediments usually are dominant in low-energy conditions with gentle slopes, such as tidal flats and protected and sheltered basins (van Rijn, 1993). Among the tested properties (Figure 6), the exposure degree of the shoreline presented the clearest relationship with SOC stocks. Significant SOC accumulation was observed only when the average fetch length 315 was smaller than approximately 500 m (Figure 6d). In these sites (Figures S1, S2 and S5), the sheltered shorelines prevent the sediments (OM and fine-grained mineral material) from being washed away, promoting their deposition and allowing a long-term storage of OC. The remaining sites, with smaller SOC stock estimates, were all located in more exposed shorelines (Figures 5d, S3, S4, S6 to S9), where the fine-grained sediments and OM are more easily carried away, for example by waves. Our results suggest that in these exposed sites, only a small amount of SOC is stored in the more surficial 320 portion of the sediments, especially in the root zone (Figures S11 to S13).

In shallow estuaries dominated by wetland vegetation, the wave activity contributes to processes such as sediment re-suspension and transport (Karimpour et al., 2017; Green and Coco, 2014). Similarly in freshwater *teal carbon* environments, waves may play an important role in sediment re-suspension and erosion from shallow vegetated shorelines. The wave



height, and hence the energy of the waves, increases with the wind speed and the fetch (the unobstructed distance over  
325 which the wind can blow) (Fagherazzi and Wiberg, 2009; Lamont-Smith and Waseda, 2007). Assuming our studied lakes are subjected to rather similar meteorological conditions, e.g. the number of days with constant wind are similar in the whole lake (Figure S24), the length of the fetch in certain direction will be the main factor controlling wave heights, with longer fetch generating waves with larger heights (Lamont-Smith and Waseda, 2007).

When taller waves (i.e., of longer fetch) reach the shoreline, their orbital motion extends to the bottom and their shear  
330 stress can exceed the critical shear stress against which the sediment resists motion. On the other hand, taller waves are more prone to breaking as they shoal, and the dissipation of wave energy in the breaker zone can erode the bottom and generate a net offshore transport (van Rijn, 1993). During this interaction, wind-induced waves tend to remove sediments from the shoreline, and fine-grained sediments tend to be washed out faster than sands. On the contrary, sheltered areas (smaller fetch) are exposed mainly to waves with smaller heights, that tend not to affect deep into the  
335 water column or break when reaching flat areas, even promoting a net onshore transport of sediments (van Rijn, 1993). The lower energy environment promotes the deposition and preservation of fine-grained sediments. Because of their high surface/volume rate and chemical charges (Keil et al., 1994; Keil and Cowie, 1999), fine-grained sediments tend to adsorb more OM and, therefore, to accumulate more organic carbon.

In addition to the shoreline exposure, we tested the effect of bathymetry on SOC accumulation. Most of the sites with SOC >  
340 10 kg SOC m<sup>-2</sup> were found around 0.5 m of water column, but one sampling site located deeper than 1.0 m water column also presented SOC stocks larger than 10 kg m<sup>-2</sup> (Figure 6b). We also studied the relationship of the shorelines' slope on average SOC stock estimates. While sites A (average of 15.6 kg m<sup>-2</sup>) and B (average of 24.7 kg m<sup>-2</sup>) are located in a region with a gentle and subtle slope (slope indices of 294 and 195, respectively), which promotes fine-grained sediments and OM accumulation, site E (average of 25.5 kg m<sup>-2</sup>) was located in the steepest  
345 site (slope index of 22) (Figure 6c).

#### 4.3 Small-scale spatial variability of SOC stocks

The spatial variability of the macrophyte belts zonation in freshwater wetlands that generally changes from more terrestrial and drier zones towards more aquatic and flooded zones has previously been described to control OC accumulation in shallow freshwater *teal carbon* ecosystems. Bernal and Mitsch (2012), Tangen and Bansal (2020) and Taran et al. (2023)  
350 found higher concentrations and stocks of OC in the inner, more aquatic portion, of the wetlands. They attribute this to the combined effect of the permanent anaerobic conditions and the high macrophyte productivity of the inner zone. Further, they observed a change in the species composition from their more landward/upper zone towards the water, which is different to what we observed in our boreal lake sites, where most macrophyte belts were monospecific. However, in a study focusing in monospecific reed belts, Buczko et al. (2022) observed larger SOC stocks in the terrestrial zone when compared to the  
355 littoral, more aquatic zone. They attributed this pattern to generally larger biomass being produced by *Phragmites* at the terrestrial edges of wetlands.



In our study, however, we did not observe any clear and general spatial pattern between SOC stocks and zones or macrophyte biomass (Figures 4c and S20). In Kallavesi, for example, the largest SOC stocks were indeed observed in the landside zone in all three sites, but the landside zone was not always the most densely vegetated. In site E, for example, the 360 largest SOC stock was observed in the landside zone, despite it having the lowest vegetation density (less than 100 stems per  $m^{-2}$ ) (Table S2, Figures 4a and S20). In Vesijärvi, the largest SOC stocks were observed in the transitional zone, with monospecific (only *Phragmites*) or mixed macrophyte belts (Figures 4a and S20). In this lake, a denser vegetation was associated with more OC accumulation, but even in the most densely vegetated study area (with almost 400 stems per  $m^{-2}$ ), the SOC stock did not exceed 10 kg TOC  $m^{-2}$  (Tables 2 and 3, Figure S20). Lake Oulujärvi had the largest SOC stocks but 365 the weakest relationship between the stocks, zones and macrophytes density (Table S2, Figures 4a and S20). In Oulujärvi, the highest stock was found in a different zone in each site. Also, the largest stock estimate we observed was found in Oulujärvi, in an area with only 62 stems per  $m^{-2}$ . This suggests that the zonation and the vegetation structure (species composition and stem density) have a secondary role in the amount of SOC stock in these *teal carbon areas* of boreal lakes. When only the more exposed areas are considered, the vegetation density had a larger role in controlling role in SOC 370 accumulation (Figure S25), possibly due to the effect of vegetation in buffering external disturbances and, subsequently, promoting the accumulation of fine-grained sediments and organic matter. Thus, although macrophyte belts, especially *Phragmites*, can thrive in a wide range of environmental conditions (Murphy, 2002), only sheltered areas of *teal carbon environments* seem to accumulate larger amounts of OC into deeper sedimentary layers.

#### 4.4 Comparison with similar vegetated environments

375 To put the *teal carbon* stocks from boreal zones in a global perspective, we compare them with the reported SOC stocks estimated for brackish and freshwater vegetated wetlands. Overall, our SOC stock estimates are well within the existing published values (Figure 7). The SOC stock estimates from Oulujärvi and Kallavesi are comparable to those observed in a monospecific *Phragmites* reed belt from coastal lagoons in northern Germany (Buczko et al., 2022) and in several freshwater marshes from southeastern Australia (Carnell et al., 2018).

380

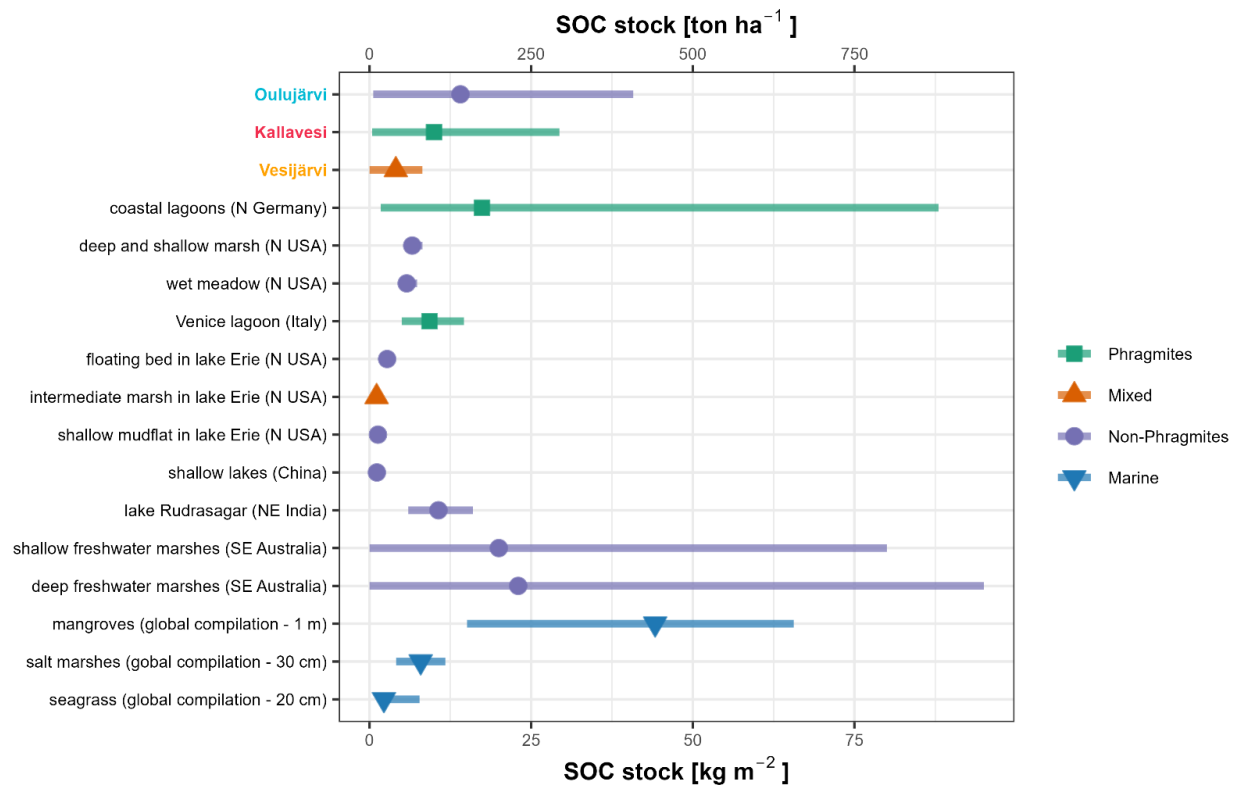


**Figure 7. Sedimentary organic carbon (SOC) stocks [kg m⁻² and ton ha⁻¹] from vegetated wetlands and shorelines (range and mean), including the Finnish study lakes. Freshwater sites are sorted by latitude. References: Buczko et al. (2022), Tangen and Bansal (2020), Silan et al. (2024), Bernal and Mitsch (2012), Wang et al. (2016), Taran et al. (2023), Carnell et al. (2018), Alongi (2022), Maxwell et al. (2023) and Kennedy et al. (2022).**

In the German coastal lagoons studied by Buczko et al. (2022), only one site (Michaelsdorf) presented organic-rich material throughout the whole sediment core (1 m length), reaching SOC stock estimates of 75 kg m⁻². For the remaining sites the SOC stock estimates ranged between 1.76 and 35 kg m⁻², and presented a clear decline in TOC content [% dw] with core depth. The Michaelsdorf sampling site is located in a relatively narrow channel connecting Saaler and Bodstedter water bodies, and is surrounded mainly by pastures. Even though the sampling site itself is not as sheltered as the sampling sites in Kallavesi (site E) and Oulujärvi (sites A and B), the geomorphology of the channel might prevent strong water currents and waves, allowing the settlement of fine-grained sediments, which in turn promotes the accumulation of TOC. Therefore, while Michaelsdorf sampling site probably stores more OC via the same mechanism as sites A, B and E in our study, the other sites in the studied German coastal lagoons probably resemble our more exposed sampling sites.

In the study by Carnell et al. (2018), data of 57 sediment cores from shallow freshwater marshes and 100 cores from deep freshwater marshes were combined. Therefore, the information about the geomorphology of each site is not



available. Carnell et al. (2018) mention, however, the influence of the proximity to major rivers. Wetlands located  
395 closer to fluvial inputs were associated with higher sediment accretion and potentially carbon sequestration. The authors point out that this might be caused by anthropogenically clearing of terrestrial vegetation in the catchment area and changes in river hydrology, leading to larger inputs of autochthonous organic matter to the adjacent wetlands and macrophyte belts.

Compared to coastal marine *blue carbon* environments (mangrove forests, salt marshes and seagrass meadows), the  
400 mean of SOC stock estimates from Oulujärvi and Kallavesi are around one third of the SOC stocks observed in mangrove forests (Alongi, 2022). When compared to salt marshes (Maxwell et al., 2023) and seagrass meadows (Kennedy et al., 2022), however, the SOC stocks from boreal *teal carbon* environments are notably larger. The overall magnitude of OC stocks observed in our study highlights the potential importance of shallow vegetated areas to OC accumulation in inland waters. Boreal latitudes contain the largest abundance of lakes in the world, especially  
405 considering lakes smaller than 0.1 km<sup>2</sup> (Verpoorter et al., 2014). Due to the high perimeter/surface area ratio of inland waters in the boreal zone, shoreline areas and associated *teal carbon* environments in boreal lakes may be important components of global C cycling.

## 5 Conclusions

This study contributes to understanding of OC burial within vegetated *teal carbon* areas from boreal lacustrine  
410 environments. A large spatial variability was observed among SOC stock estimates from the three studied lakes, and larger OC accumulation was only observed in the presence of fine-grained sediments. Most of the sampling sites presented a relatively thin layer of organic-rich material on the surface, followed by organic-poor material deeper in the sediment cores. The sites where the organic-rich material extended through the whole core were all located in sheltered basins. In those areas, the sheltered shoreline prevents sediments, and consequently OM, from being washed away, promoting OC  
415 accumulation. Thus, although macrophyte belts, especially *Phragmites*, can thrive in a wide range of environmental conditions, only sheltered areas seem to accumulate larger amounts of OC into deeper sedimentary layers. In more exposed areas, however, the vegetation density might play an additional controlling role in SOC accumulation, partly corroborating our first hypothesis. The presence of vegetation is likely to buffer external disturbances and, subsequently, promote the accumulation of fine-grained sediments and organic matter in these more exposed  
420 shorelines.

Identifying the major controlling factors of OC cycling and accurately determining the importance of vegetated shallow areas from inland waters to OC (accumulation) stocks is essential for constraining regional OC budgets. Boreal zones contain a high abundance of lakes, and despite their relatively small areas, these *teal carbon* ecosystems can contribute significantly to the OC cycling, possibly as much as some *blue carbon* ecosystems, thus corroborating the second hypothesis  
425 of this study.



## Data availability

All new data presented in the paper are accessible as Supplementary Material, via Pangaea (<https://doi.org/10.1594/PANGAEA.986726> and <https://doi.org/10.1594/PANGAEA.986727>) or directly from the corresponding author without undue reservation.

## 430 Supplement

Supplemental material is supplied as a separate file.

## Author contributions

TJ, KK and MJ designed the concept of the study. SV provided the images showing evidence of extensive areas of macrophyte vegetation on Finnish lakes used in the sampling delineation. AD and MK processed the laboratory analysis. EA 435 participated in the data analysis. AD performed the statistical analysis and wrote the first draft of the manuscript. All authors contributed to manuscript writing and commenting, and approved the submitted version.

## Competing interests

The authors declare that they have no conflict of interest.

## Acknowledgements

440 The authors would like to thank everyone that helped in the field campaign, especially Matti Laatikainen and Tuomas Junna.  
The authors also acknowledge Marie Korpo for the constructive discussions.

## Financial support

This work was supported by a 3-year consortium project funded by EU Resilience and Recovery Facility (RRF) via 445 Academy of Finland / Research Council of Finland (“BlueLakes: digitizing the carbon sink potential of boreal lakes”, grant 353317). The data in this study are a contribution from the Tvarminne Zoological Station (grain size analysis) and from the geophysical, environmental and mineralogical laboratories (HelLabs) of the Department of Geology and Geophysics (organic matter analysis), both from the University of Helsinki. Open access was funded by Helsinki University Library.



## References

Alongi, D. M.: Impacts of climate change on Blue Carbon stocks and fluxes in mangrove forests, *Forests*, 13, 149, 450 <https://doi.org/10.3390/f13020149>, 2022.

Järvi-meriwiki: Oulujärvi: [https://www.jarviwiki.fi/wiki/Oulujärvi\\_\(yhd.\)](https://www.jarviwiki.fi/wiki/Oulujärvi_(yhd.)), last access: 29 September 2025.

Bernal, B. and Mitsch, W. J.: Comparing carbon sequestration in temperate freshwater wetland communities, *Glob. Chang. Biol.*, 18, 1636–1647, <https://doi.org/10.1111/j.1365-2486.2011.02619.x>, 2012.

Bianchi, T. S.: Biogeochemistry of estuaries, 1st ed., Oxford University Press, New York, U.S.A., 721 pp., 2007.

455 Bornette, G. and Puijalon, S.: Macrophytes: Ecology of aquatic plants, *Encycl. Life Sci.*, <https://doi.org/https://doi.org/10.1002/9780470015902.a0020475>, 2009.

Buczko, U., Jurasinski, G., Glatzel, S., and Karstens, S.: Blue carbon in coastal Phragmites wetlands along the southern Baltic Sea, *Estuaries and Coasts*, 45, 2274–2282, <https://doi.org/10.1007/s12237-022-01085-7>, 2022.

Burdige, D. J. (Ed.): Physical properties of sediments, in: *Geochemistry of Marine Sediments*, Princeton University Press, 460 New Jersey, 624, 2006.

Carnell, P. E., Windecker, S. M., Brenker, M., Baldock, J., Masque, P., Brunt, K., and Macreadie, P. I.: Carbon stocks, sequestration, and emissions of wetlands in south eastern Australia, *Glob. Chang. Biol.*, 24, 4173–4184, <https://doi.org/10.1111/gcb.14319>, 2018.

Cole, J. J., Prairie, Y. T., Caraco, N. F., McDowell, W. H., Tranvik, L. J., Striegl, R. G., Duarte, C. M., Kortelainen, P., 465 Downing, J. A., Middelburg, J. J., and Melack, J.: Plumbing the global carbon cycle: Integrating inland waters into the terrestrial carbon budget, *Ecosystems*, 10, 171–184, <https://doi.org/10.1007/s10021-006-9013-8>, 2007.

Convention on Wetlands: Global Wetland Outlook: Special Edition 2021, edited by: Dudley, N., Secretariat of the Convention on Wetlands, Gland, Switzerland, 98–100 pp., <https://doi.org/10.2307/jj.9561408.32>, 2021.

Duarte, C. M., Middelburg, J. J., and Caraco, N. F.: Major role of marine vegetation on the oceanic carbon cycle C, 470 *Biogeosciences*, 2, 1–8, <https://doi.org/10.5194/bg-2-1-2005>, 2005.

DVV (Digi- ja väestötietovirasto; Digital and Population Information Agency of Finland): Finland shapefile: <https://www.avoindata.fi/data/fi/dataset/suomen-maakunnat-2021-vuoden-2018-maakuntakoodeilla/resource/3c2a8036-e774-458a-810a-2c1fc0f80d5f>, last access: 25 May 2023.

Fagherazzi, S. and Wiberg, P. L.: Importance of wind conditions, fetch, and water levels on wave-generated shear stresses in 475 shallow intertidal basins, *J. Geophys. Res. Earth Surf.*, 114, F03022, <https://doi.org/10.1029/2008JF001139>, 2009.

FMI (Finnish Meteorological Institute) database: <https://en.ilmatieteenlaitos.fi/download-observations>, last access: 9 August 2024.

Glückert, G.: On deglaciation between Pieksämäki and Pielavesi in central Finland, *Bull. Geol. Soc. Finl.*, 46, 43–51, <https://doi.org/10.17741/bgsf/46.1.007>, 1974.

480 Grasset, C., Mesman, J. P., Tranvik, L. J., Maranger, R., and Sobek, S.: Contribution of lake littoral zones to the continental



carbon budget, *Nat. Geosci.*, 18, 747–752, <https://doi.org/10.1038/s41561-025-01739-8>, 2025.

Green, M. O. and Coco, G.: Review of wave-driven sediment resuspension and transport in estuaries *Reviews of Geophysics*, *Eos, Trans. Am. Geophys.* ..., 52, 77–117, <https://doi.org/10.1002/2013RG000437>, 2014.

GTK (Geological Survey of Finland): Maankamara: <https://gtkdata GTK.fi/maankamara/>, last access: 3 April 2024.

485 Hayes, M. O.: An exposure index for oiled shorelines, *Spill Sci. Technol. Bull.*, 3, 139–147, [https://doi.org/10.1016/S1353-2561\(96\)00014-X](https://doi.org/10.1016/S1353-2561(96)00014-X), 1996.

Hijmans, R. J., Bivand, R., Cordano, E., Dyba, K., Pebesma, E., and Sumner, M. D.: *terra: Spatial Data Analysis*. R package version 1.7-83, <https://cran.r-project.org/web/packages/terra/index.html>, 2024.

Hyvärinen, H.: The deglaciation history of eastern Fennoscandia - recent data from Finland, *Boreas*, 2, 85–102, 490 <https://doi.org/10.1111/j.1502-3885.1973.tb00975.x>, 1973.

Junna, T., Asmala, E., Mäkinen, J., Kortelainen, P., Jilbert, T., and Koho, K.: Land use as a key driver of increased organic carbon burial in boreal lakes, *Biogeochemistry*, *in press*.

Kairesalo, T. and Vakkilainen, K.: Lake Vesijärvi and the City of Lahti (southern Finland) comprehensive interactions between the lake and the coupled human community, *SIL news*, 41, 1–12, 2004.

495 Kankaala, P., Ojala, A., and Käki, T.: Temporal and spatial variation in methane emissions from a flooded transgression shore of a boreal lake, *Biogeochemistry*, 68, 297–311, <https://doi.org/10.1023/B:BIOG.0000031030.77498.1f>, 2004.

Karimpour, A., Chen, Q., and Twilley, R. R.: Wind wave behavior in fetch and depth limited estuaries, *Sci. Rep.*, 7, 40654, <https://doi.org/10.1038/srep40654>, 2017.

500 Keil, R. G. and Cowie, G. L.: Organic matter preservation through the oxygen-deficient zone of the NE Arabian Sea as discerned by organic carbon:mineral surface area ratios, *Mar. Geol.*, 161, 13–22, [https://doi.org/10.1016/S0025-3227\(99\)00052-3](https://doi.org/10.1016/S0025-3227(99)00052-3), 1999.

Keil, R. G., Montluçon, D. B., Prahl, F. G., and Hedges, J. I.: Sorptive preservation of labile organic matter in marine sediments, *Lett. to Nat.*, 370, 549–551, 1994.

505 Kennedy, H., Pagès, J. F., Lagomasino, D., Arias-Ortiz, A., Colarusso, P., Fourqurean, J. W., Githaiga, M. N., Howard, J. L., Krause-Jensen, D., Kuwae, T., Lavery, P. S., Macreadie, P. I., Marbà, N., Masqué, P., Mazarrasa, I., Miyajima, T., Serrano, O., and Duarte, C. M.: Species traits and geomorphic setting as drivers of global soil carbon stocks in seagrass meadows, *Global Biogeochem. Cycles*, 36, 1–18, <https://doi.org/10.1029/2022GB007481>, 2022.

Keränen, R., Riihimäki, J., Asunmaa, A., Madekivi, O., Hellsten, S., Alasaarela, E., and Seppänen, E.: *Oulujärven rantojen kasvillisuuden kehittyminen ja käyttöedellytysten parantaminen, Vesi- ja ympäristöhallituksen monistesarja*, Helsinki, 510 104 pp., 1992.

Koponen, S., Väkevä, S., Jokinen, A.-P., Virtanen, E., Viitasalo, M., Blenckner, T., and Cervo, A. de: *Blue Carbon Habitats - a comprehensive mapping of Nordic salt marshes for estimating Blue Carbon storage potential*, <https://doi.org/10.6027/temanord2022-506>, 2022.

Kortelainen, P., Pajunen, H., Rantakari, M., and Saarnisto, M.: A large carbon pool and small sink in boreal Holocene lake



515 sediments, *Glob. Chang. Biol.*, 10, 1648–1653, <https://doi.org/10.1111/j.1365-2486.2004.00848.x>, 2004.

Lamont-Smith, T. and Waseda, T.: Wind wave growth at short fetch, *J. Phys. Oceanogr.*, 38, 1597–1606, <https://doi.org/10.1175/2007JPO3712.1>, 2007.

Leonard, L. A. and Luther, M. E.: Flow hydrodynamics in tidal marsh canopies, *Limnol. Oceanogr.*, 40, 1474–1484, <https://doi.org/10.4319/lo.1995.40.8.1474>, 1995.

520 Leonard, L. A., Wren, P. A., and Beavers, R. L.: Flow dynamics and sedimentation in *Spartina alterniflora* and *Phragmites australis* marshes of the Chesapeake Bay, *Wetlands*, 22, 415–424, [https://doi.org/10.1672/0277-5212\(2002\)022\[0415:FDASIS\]2.0.CO;2](https://doi.org/10.1672/0277-5212(2002)022[0415:FDASIS]2.0.CO;2), 2002.

Li, H. and Yang, S. L.: Trapping effect of tidal marsh vegetation on suspended sediment, Yangtze Delta, *J. Coast. Res.*, 25, 915–924, <https://doi.org/10.2112/08-1010.1>, 2009.

525 Lunkka, J. P., Ojala, A. E. K., Kaakinen, A., Hovikoski, J., Kultti, S., Kuosmanen, N., Palmu, J. P., Putkinen, N., Sarala, P., and Virtasalo, J.: Stratigraphic framework for the classification of Quaternary deosits in Finland, *Geol. Surv. Finl. Bull.*, 418, 77–143, 2024.

Marchand, P. and Gill, D.: waver: Calculate Fetch and Wave Energy. R package version 0.3.0, <https://cran.r-project.org/web/packages/waver/index.html>, 2023.

530 Marschner, I. and Donoghoe, M. W.: glm2: Fitting Generalized Linear Models. R package version 1.2.1, <https://cran.r-project.org/web/packages/glm2/index.html>, 2022.

Maxwell, T. L., Rovai, A. S., Adame, M. F., Adams, J. B., Álvarez-Rogel, J., Austin, W. E. N., Beasy, K., Boscutti, F., Böttcher, M. E., Bouma, T. J., Bulmer, R. H., Burden, A., Burke, S. A., Camacho, S., Chaudhary, D. R., Chmura, G. L., Copertino, M., Cott, G. M., Craft, C., Day, J., de los Santos, C. B., Denis, L., Ding, W., Ellison, J. C., Ewers 535 Lewis, C. J., Giani, L., Gispert, M., Gonharet, S., González-Pérez, J. A., González-Alcaraz, M. N., Gorham, C., Graversen, A. E. L., Grey, A., Guerra, R., He, Q., Holmquist, J. R., Jones, A. R., Juanes, J. A., Kelleher, B. P., Kohfeld, K. E., Krause-Jensen, D., Lafratta, A., Lavery, P. S., Laws, E. A., Leiva-Dueñas, C., Loh, P. S., Lovelock, C. E., Lundquist, C. J., Macreadie, P. I., Mazarrasa, I., Megonigal, J. P., Neto, J. M., Nogueira, J., Osland, M. J., Pagès, J. F., Perera, N., Pfeiffer, E. M., Pollmann, T., Raw, J. L., Recio, M., Ruiz-Fernández, A. C., Russell, S. K., 540 Rybczyk, J. M., Sammul, M., Sanders, C., Santos, R., Serrano, O., Siewert, M., Smeaton, C., Song, Z., Trasar-Cepeda, C., Twilley, R. R., Van de Broek, M., Vitti, S., Antisari, L. V., Voltz, B., Wails, C. N., Ward, R. D., Ward, M., Wolfe, J., Yang, R., Zubrzycki, S., Landis, E., Smart, L., Spalding, M., and Worthington, T. A.: Global dataset of soil organic carbon in tidal marshes, *Sci. Data*, 10, 797, <https://doi.org/10.1038/s41597-023-02633-x>, 2023.

Mendonça, R., Müller, R. A., Clow, D., Verpoorter, C., Raymond, P., Tranvik, L. J., and Sobek, S.: Organic carbon burial in 545 global lakes and reservoirs, *Nat. Commun.*, 8, 1–6, <https://doi.org/10.1038/s41467-017-01789-6>, 2017.

Milliman, J. D.: Organic matter content in U.S. Atlantic continental slope sediments: Decoupling the grain-size factor, *Deep. Res. Part II*, 41, 797–808, [https://doi.org/10.1016/0967-0645\(94\)90049-3](https://doi.org/10.1016/0967-0645(94)90049-3), 1994.

Mohamed Anas, M. U., Scott, K. A., and Wissel, B.: Carbon budgets of boreal lakes: state of knowledge, challenges, and



implications, *Environ. Rev.*, 23, 275–287, 2015.

550 Murphy, K. J.: Plant communities and plant diversity in softwater lakes of northern Europe, *Aquat. Bot.*, 73, 287–324, [https://doi.org/10.1016/S0304-3770\(02\)00028-1](https://doi.org/10.1016/S0304-3770(02)00028-1), 2002.

Murtojärvi, M., Suominen, T., Tolvanen, H., Leppänen, V., and Nevalainen, O. S.: Quantifying distances from points to polygons-applications in determining fetch in coastal environments, *Comput. Geosci.*, 33, 843–852, <https://doi.org/10.1016/j.cageo.2006.10.006>, 2007.

555 Nahlik, A. M. and Fennessy, M. S.: Carbon storage in US wetlands, *Nat. Commun.*, 7, 1–9, <https://doi.org/10.1038/ncomms13835>, 2016.

Nikora, V., Larned, S., Debnath, K., Cooper, G., and Reid, M.: Hydraulic resistance due to aquatic vegetation in small streams: Field study, *J. Hydraul. Eng.*, 134, 1326–1332, [https://doi.org/10.1061/\(ASCE\)0733-9429\(2008\)134](https://doi.org/10.1061/(ASCE)0733-9429(2008)134), 2008.

Noori, R., Bateni, S. M., Saari, M., Almazroui, M., and Torabi Haghghi, A.: Strong warming rates in the surface and bottom 560 layers of a boreal lake: Results from approximately six decades of measurements (1964–2020), *Earth Sp. Sci.*, 9, <https://doi.org/10.1029/2021EA001973>, 2022.

Ojala, A. E. K., Luoto, T. P., and Virtasalo, J. J.: Establishing a high-resolution surface sediment chronology with multiple dating methods – Testing  $^{137}\text{Cs}$  determination with Nurmijärvi clastic-biogenic varves, *Quat. Geochronol.*, 37, 32–41, <https://doi.org/10.1016/j.quageo.2016.10.005>, 2017.

565 Finnish National Geoportal (Orthophotos): <https://kartta.paikkatietoikkuna.fi/?lang=en>, last access: 17 July 2023.

Pajunen, H.: Carbon in Finnish lake sediments, Espoo, 2000.

Partanen, S., Keto, A., Visuri, M., Tarvainen, A., Riihimäki, J., and Hellsten, S.: The relationship between water level fluctuation and distribution of emergent aquatic macrophytes in large, mildly regulated lakes in the Finnish Lake District, *SIL Proceedings, 1922-2010*, 29, 1160–1166, <https://doi.org/10.1080/03680770.2005.11902867>, 2006.

570 QGIS Development Team: QGIS Geographic Information System. Open Source Geospatial Foundation Project. Version 3.28.4-Firenze, <http://qgis.org>, 2024.

R Core Team: R: A language and environment for statistical computing (version 4.3.3), <https://www.r-project.org/>, 2024.

Rainio, H., Saarnisto, M., and Ekman, I.: Younger Dryas end moraines in Finland and NW Russia, *Quat. Int.*, 28, 179–192, [https://doi.org/10.1016/1040-6182\(95\)00051-J](https://doi.org/10.1016/1040-6182(95)00051-J), 1995.

575 Regnier, P., Resplandy, L., Najjar, R. G., and Cai, P.: The land-to-ocean loops of the global carbon cycle, *Nature*, 603, 401–410, <https://doi.org/10.1038/s41586-021-04339-9>, 2022.

Repo, R. and Tynni, R.: Observations on the Quaternary geology of an area between the 2nd Salpausselkä and the ice-marginal formation of central Finland, *Bull. Geol. Soc. Finl.*, 43, 185–202, <https://doi.org/10.17741/bgsf/43.2.005>, 1971.

580 van Rijn, L. C.: Principles of sediment transport in rivers, estuaries and coastal seas, Aqua Publications, Amsterdam, 690 pp., 1993.

Silan, G., Buosi, A., Bertolini, C., and Sfriso, A.: Dynamics and drivers of carbon sequestration and storage capacity in



Phragmites australis-dominated wetlands, Estuar. Coast. Shelf Sci., 298, 108640,

<https://doi.org/10.1016/j.ecss.2024.108640>, 2024.

585 Syke (Finnish Environmental Institute): Ecological status of surface waters 2019 - Finland, 2019.

Syke (Finnish Environmental Institute): VALUE - valuma-alueen rajaustyökalu (watershed delineation tool): <https://paikkatieto.ymparisto.fi/value/>, last access: 21 January 2025a.

Syke (Finnish Environmental Institute): Hertta database of Syke, 3rd River Basin Management Plan, data from 2012-2017: [https://www.syke.fi/fi-fi/avoin\\_tieto/ymparistotietojarjestelmat](https://www.syke.fi/fi-fi/avoin_tieto/ymparistotietojarjestelmat), last access: 21 January 2025b.

590 Tangen, B. A. and Bansal, S.: Soil organic carbon stocks and sequestration rates of inland, freshwater wetlands: Sources of variability and uncertainty, *Sci. Total Environ.*, 749, 141444, <https://doi.org/10.1016/j.scitotenv.2020.141444>, 2020.

Taran, M., Ahirwal, J., Deb, S., and Sahoo, U. K.: Variability of carbon stored in inland freshwater wetland in Northeast India, *Sci. Total Environ.*, 859, 160384, <https://doi.org/10.1016/j.scitotenv.2022.160384>, 2023.

Tikkanen, M.: The changing landforms of Finland, *Fennia*, 180, 21–30, 2002.

595 Tikkanen, M.: The landforms of Finland, in: Finland - land of mires, edited by: Lindholm, T. and Heikkilä, R., Finnish Environment Institute, 27–38, 2006.

Tranvik, L. J., Cole, J. J., and Prairie, Y. T.: The study of carbon in inland waters—from isolated ecosystems to players in the global carbon cycle, *Limnol. Oceanogr. Lett.*, 3, 41–48, <https://doi.org/10.1002/lol2.10068>, 2018.

600 Turunen, J., Hellsten, S., and Marttunen, M.: Oulujoen vesistöalueen säännös- teltyjen järvienväistely- suositusten toteutuminen. ARVOVESI-hankkeen raportti 5, 1–63 pp., 2022.

Verpoorter, C., Kutser, T., Seekell, D. A., and Tranvik, L. J.: A global inventory of lakes based on high-resolution satellite imagery, *Geophys. Res. Lett.*, 41, 6396–6402, <https://doi.org/10.1002/2014GL060641>, 2014.

Wang, H. J., Wang, H. Z., Liang, X. M., Pan, B. Z., and Kosten, S.: Macrophyte species strongly affects changes in C, N, and P stocks in shallow lakes after a regime shift from macrophyte to phytoplankton dominance, *Inl. Waters*, 6, 449–460, <https://doi.org/10.1080/IW-6.3.837>, 2016.

605 Wickham, H.: *ggplot2: Elegant Graphics for Data Analysis*. R package version 3.5.0, Springer-Verlag New York, 2016.